59th ILMENAU SCIENTIFIC COLLOQUIUM
Technische Universität Ilmenau, 11 — 15 September 2017
URN: urn:nbn:de:gbv:ilm1-2017iwk-048:9

CONTROL OF COMPLIANT ROBOTIC SYSTEMS WITH MUSCLE-LIKE ACTUATORS AND SATURATED FEEDBACK

Konrad Siedler / Carsten Behn

Technical Mechanics Group, Department of Mechanical Engineering
Technische Universität Ilmenau
Max-Planck-Ring 12, 98693 Ilmenau, Germany
}konrad.siedler, carsten.behn‖@tu-ilmenau.de

ABSTRACT

This paper is devoted to the problem in controlling a compliant robotic system by means of actuators with muscle-like properties, which underlie prescribed bounds due to the natural muscle behavior. A typical example to demonstrate the effectiveness of developed control schemes is the choice of a (inverted) pendulum with higher degree of freedom. Due to the force restriction of the driving muscle forces, we have to sought (saturated) feedback strategies to control the system behavior (e.g. tracking of paths) which have to be limited a-priori. A suitable control variable can be generated by adaptive controllers, e.g., a PID-λ-stabilization. But, the classical torque control variable has to be converted to the muscle force at the joints, and the joint angle velocity has to be converted to the contraction velocity. The effective force at every joint is the difference of the antagonistic muscles pairs with the muscle characteristic curve of HILL (force-velocity-relation). The aim is now, to hold the control variable inside the area restricted by the muscle pairs. Several simulations show the effectiveness of the designed controllers.

Index Terms— compliant system, muscle force, muscle-like actuator, adaptive control, saturated feedback.

1. INTRODUCTION

Today, artificial muscles are a serious alternative to conventional motors, especially for systems in which the moving elements do not have to perform a whole revolution. This paper is devoted to the problem in controlling a compliant robotic system by means of actuators with muscle-like properties, which underlie prescribed bounds due to the natural muscle behavior. To avoid damage to the actuators and ensure the system behavior, saturated feedback strategies are necessary. Due to the compliance of the system, many parameters are unknown and/or uncertain, why adaptive control strategies are chosen. A typical example to demonstrate the effectiveness of developed control schemes is the choice of a (inverted) pendulum with $DoF \in 2$, see [2] and [6].

2. MATHEMATICAL MODEL

To analyze these adaptive control strategies a model is chosen, in which the artificial, compliant muscles are meaningful implemented with a sufficient number of inaccuracies. For this, a biological inspired robot arm in form of a double pendulum (simplified SCARA-type) with two antagonistic muscle pairs is chosen. The functional principle and the mechanical quantities of the system are depicted in Fig. 1. Using this model, the efficiency of the designed control strategies should be well visible.

m_i mass of element
J_i mass moment of inertia w.r.t. to s_i
s_i center of mass m_i
l_i distances between joints
r_i distances between center of masses
ϑ_i (relative) angle of pivot joint
$C_{C\,k}$ contractile muscle-like element

for i = 1,2
k = 1 ... 4

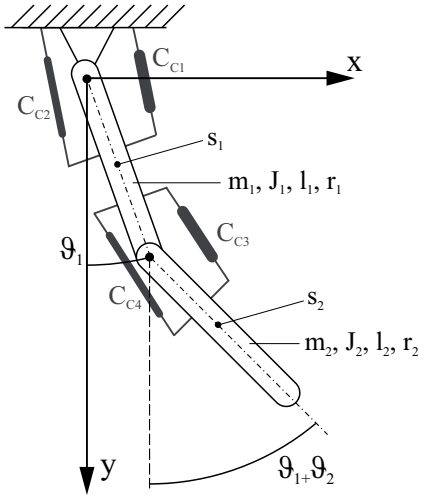

Figure 1. Underlying double pendulum structure with actuator arrangement.

To determine the equations of motion, we use the Euler-Lagrange equations of the 2nd kind with the generalized coordinates $q_1 := \vartheta_1$ and $q_2 := \vartheta_2$. The following matrix-vector notation results [1]:

$$M(q)\ddot{q} + C(q,\dot{q})\dot{q} + G(q) = u, \tag{1}$$

with:

$$\begin{aligned}
M(q) &= \begin{pmatrix} m_1\, r_1^2 + J_1 + m_2\left[l_1^2 + r_2^2 + 2\, l_1\, r_2 \cos(q_2)\right] + J_2 & m_2\left[r_2^2 + l_1\, r_2 \cos(q_2)\right] + J_2 \\ m_2\left[r_2^2 + l_1\, r_2 \cos(q_2)\right] + J_2 & m_2\, r_2^2 + J_2 \end{pmatrix}, \\
C(q,\dot{q})\,\dot{q} &= \begin{pmatrix} m_2\, l_1\, r_2 \sin(q_2)\left[\dot{q}_2^2 + 2\dot{q}_1\,\dot{q}_2\right] \\ \dot{q}_1^2\, m_2\, l_1\, r_2 \sin(q_2) \end{pmatrix}, \\
G(q) &= \begin{pmatrix} \sin(q_1)[m_1\, g\, r_1 + m_2\, g\, l_1] + m_2\, g\, r_2 \sin(q_1 + q_2) \\ m_2\, g\, r_2 \sin(q_1 + q_2) \end{pmatrix}
\end{aligned} \tag{2}$$

3. CONTROL STRATEGIES

As mentioned above, we have to deal with uncertainties, i.e., the system parameters are not known or are uncertain. Hence, primarily adaptive control strategies are chosen. The tuning of the gain parameters (by trial&error-methods) of conventional PID-strategies will consume a lot of time:

$$\left.\begin{aligned}
e_i(t) &:= q_i(t) \quad q_{Ref\,i}(t) \\
u_i(t) &= \underbrace{k_{Pi}\, e_i(t)}_{P-part} \quad \underbrace{k_{Di}\,\kappa_i\,\dot{e}_i(t)}_{D-part} \quad \underbrace{k_{Ii}\,\eta_i \int_0^t e_i(t)dt}_{I-part} \\
&\text{with } k_{Pi}, k_{Di}, k_{Ii} \wedge \mathbb{R}
\end{aligned}\right\} \tag{3}$$

Remark: The index i in the following control strategies indicates the two control inputs at the joint $i = 1, 2$ of the model.

A way out of this problem is the choice of adaptive controllers – having time-variant gain parameters which adjust their necessary control values on their own using some adaptation laws. More precisely, a simple control objective is the λ-stabilization one. It allows the design of simple feedback strategies, as described in the following:

$$\left.\begin{aligned}
e_i(t) &:= q_i(t) \quad q_{Ref\,i}(t) \\
u_i(t) &= \quad k_i(t)\, e_i(t) \quad \kappa_i\, k_i(t)\,\dot{e}_i(t) \quad \eta_i\, k_i(t) \int_0^t e_i(t)dt \\
\dot{k}_i(t) &= \begin{cases} \gamma_i\,(\ e_i(t) \quad \lambda_i)^2 & \text{for} \quad e_i(t) \ \in \lambda_i \\ 0 & \text{else} \end{cases}
\end{aligned}\right\} \tag{4}$$

Using this control strategy, a so-called λ-tolerance area is introduced, in which the error value of the system is accepted/tolerated. Outside of this area the gain factor will rise up in dependence on the deviation to the tolerance area. The factor γ describes a proportional factor to gain the growth of the gain factor.
A more specialized control strategy is the advanced λ-stabilization, which is derived from (4), [5]:

$$\left.\begin{array}{l} e_i(t) := q_i(t) \quad q_{Ref\,i}(t) \\ u_i(t) = \quad k_i(t)\, e_i(t) \quad \kappa_i\, k_i(t)\, \dot{e}_i(t) \quad \eta_i\, k_i(t) \int_0^t e_i(t)dt \\ \dot{k}_i(t) \quad = \gamma_i \left\{ \begin{array}{ll} (\ e_i(t) \quad \varepsilon_i\lambda_i)^2 & \text{for} \quad \varepsilon_i\lambda_i + 1 \geq \ e_i(t) \\ (\ e_i(t) \quad \varepsilon_i\lambda_i)^{\frac{1}{2}} & \text{for} \quad \varepsilon_i\lambda_i \geq \ e_i(t) \ < \varepsilon_i\lambda_i + 1 \\ 0 & \text{for} \quad e_i(t) \ < \varepsilon_i\lambda_i \ \{ \ t \quad t_{ei} < t_{di} \\ \delta_i(\ e_i(t) \ , \varepsilon_i\lambda_i)\, k_i(t) & \text{for} \quad e_i(t) \ < \varepsilon_i\lambda_i \ \{ \ t \quad t_{ei} \in t_{di} \end{array} \right. \\ \qquad \text{with } \delta_i(\ e_i(t) \ , \varepsilon_i\lambda_i) := \sigma_i\left(1 \quad \frac{e_i(t)}{\varepsilon_i\lambda_i}\right) \end{array}\right\} \tag{5}$$

with some additional parameters:

ε	-	proportional factor to force the gain factor to rise up *before* the error value leaves the tolerance area;
$\delta(\lesssim$	-	function to reduce the gain factor;
t_e	-	time stamp, when the system value enters the tolerance area;
t_d	-	time how long the system value has to stay in the tolerance area, before the gain factor will be reduced by δ.

A third control strategy, just for comparison with previous results is a saturated control strategy from the very beginning. This one was derived in [1], it is adapted from [7]. It works by compensating the potential energy of the system:

$$\left.\begin{array}{l} e_i(t) := q_{pi}(t) \quad q_{di}(t) \\ \dot{q}_{ci}(t) = \quad k_{1i}\, q_{ci}(t) \quad k_{2i}\, \text{sat}(q_{ci}(t) \quad e_i(t)) \\ u_{pi}(t) = k_{2i}\, \text{sat}(q_{ci}(t) \quad e_i(t)) + \dfrac{\partial}{\partial q_{pi}(t)}\, U_p(q_p(t)) \\ \text{with } U_p(q_p(t)) = (\ \ m_1\, g\, r_1 \quad m_2\, g\, l_1)\, \cos(q_{p1}(t)) \quad m_2\, g\, r_2\, \cos(q_{p1}(t) + q_{p2}(t)) \end{array}\right\} \tag{6}$$

4. SATURATION OF THE FEEDBACK

To ensure a non-destructive operating, the system needs a saturated control variable u. Therefore, the muscle characteristic curve of HILL (force-velocity-relation) is used [8]. Then, the maximum possible muscle force is faced to the contraction velocity $\dot{S}$. This relation can be described by the approximation [1]:

$$h_j(\lesssim = a_j^* \quad b_j^* \arctan(c_j^* \lesssim) \qquad \text{with } a_j^*, b_j^*, c_j^* \wedge \mathbb{R}, j = 1, \ldots, 4 \tag{7}$$

The index j describes each muscle C_{Cj} of the system $j = 1, \ldots, 4$. The needed muscle force F_i can be interpreted as a percentage of the possible maximum power – this ratio is called *intensity* v_j [11]:

$$F_j = v_j\, h_j(\lesssim \tag{8}$$

The effective force on every joint is the difference of the antagonistic muscles pairs [1]:

$$F_1 = v_1\, h_1(\dot{S}_1) \quad v_2\, h_2(\ \ \dot{S}_1), \quad F_2 = v_3\, h_3(\dot{S}_2) \quad v_4\, h_4(\ \ \dot{S}_2) \tag{9}$$

As a consequence now, the control input variable u_i has to be converted to the muscle forces F_i, and the joint angle velocity $\dot{q}_i$ has to be converted to the contraction velocity $\dot{S}_i$, with $i = 1, 2$, see [9].
To calculate the necessary muscle force the mechanical properties are respected, i.e., the joint of the limb elements are positioned at the height of the muscle's joints:

$$F_i(t) = \frac{u_i(t)}{a_i\, \cos(q_i)}\,, \tag{10}$$

introducing the variable a_i which describes the distance between joint of the limb elements and the muscle's joints. The contraction velocity $\dot{S}_i$ is then

$$\dot{S}_i = a_i \, \dot{q}_i \, \cos(q_i). \tag{11}$$

The task is now, to hold the control variable in an area restricted by the $h(\measuredangle$-functions of the muscle pairs, see (9). One way in doing this is, that the controller variables are chosen to stay in this area (maybe by a trial&error-method). More promising, the control variable can be saturated so that no higher values of the control variable is allowed than the system can process. With the saturated controller (6) this behavior is already included. The others (3) to (5) need a hard "cut-off", so following saturation is included for the following simulations:

$$\begin{array}{l} h_2(\ \ \dot{S}_1) v_2 \in F_1 \geq h_1(\dot{S}_1) v_1 \quad \text{with } v_1 = 1 \text{ for } F_1 > h_1(\dot{S}_1) \text{ and } v_2 = 1 \text{ for } F_1 < \quad h_2(\ \ \dot{S}_1) \\ h_4(\ \ \dot{S}_2) v_4 \in F_2 \geq h_3(\dot{S}_2) v_3 \quad \text{with } v_3 = 1 \text{ for } F_2 > h_3(\dot{S}_2) \text{ and } v_4 = 1 \text{ for } F_2 < \quad h_4(\ \ \dot{S}_2) \end{array} \tag{12}$$

To solve (9) and get usable muscle intensities, we introduce the following complimentary-slackness conditions which is very easy to be implemented:

$$v_1 \, v_2 = 0; \quad v_3 \, v_4 = 0 \tag{13}$$

This was done and analyzed in [1]. A much more specified system of such rules can reflect the real model much better. So the following rules are implemented to active the contra muscle for a moving to the course against the intended one. Additionally, the factor ξ allows to switch this behavior to the movement of a segment by a relaxation of the active muscle, so that the targeted position can be reached more stable. The following law shows rules for the first segment, the same holds for the second one, [9]:

$$\left.\begin{array}{llllll}
\text{for} & \cos(q) > 0\,, & \dot{q}_1 > \xi_1\,, & F_1 > 0: & v_1 = \dfrac{F_1}{h_1(\dot{S}_1)}\,, & v_2 = 0 \\
\text{for} & \cos(q) > 0\,, & \dot{q}_1 > \quad \xi_1\,, & F_1 < 0: & v_1 = \dfrac{F_1}{h_1(\ \ \dot{S}_1)}\,, & v_2 = 0 \\
\text{for} & \cos(q) > 0\,, & \dot{q}_1 < \xi_1\,, & F_1 > 0: & v_1 = 0\,, & v_2 = \dfrac{F_2}{h_2(\dot{S}_1)} \\
\text{for} & \cos(q) > 0\,, & \dot{q}_1 < \quad \xi_1\,, & F_1 < 0: & v_1 = 0\,, & v_2 = \dfrac{F_2}{h_2(\ \ \dot{S}_1)} \\
\text{for} & \cos(q) < 0\,, & \dot{q}_1 > \xi_1\,, & F_1 > 0: & v_1 = 0\,, & v_2 = \dfrac{F_2}{h_2(\dot{S}_1)} \\
\text{for} & \cos(q) < 0\,, & \dot{q}_1 > \quad \xi_1\,, & F_1 < 0: & v_1 = 0\,, & v_2 = \dfrac{F_2}{h_2(\ \ \dot{S}_1)} \\
\text{for} & \cos(q) < 0\,, & \dot{q}_1 < \xi_1\,, & F_1 > 0: & v_1 = \dfrac{F_1}{h_1(\dot{S}_1)}\,, & v_2 = 0 \\
\text{for} & \cos(q) < 0\,, & \dot{q}_1 < \quad \xi_1\,, & F_1 < 0: & v_1 = \dfrac{F_1}{h_1(\ \ \dot{S}_1)}\,, & v_2 = 0
\end{array}\right\} \tag{14}$$

5. SIMULATIONS

In several simulations the following system quantities are presented in figures: the angles q_i, the forces F_i, the intensities v_j, and the controller restrictions $F_i(\dot{S}_i)$, with $i = 1, 2$ and $j = 1 \ldots 4$. Further, the follwing system parameter are chosen for all simulations, oriented to [9]:

$$\begin{array}{llll} m_1 = m_2 = 2 & r_1 = r_2 = 1 & l_1 = l_2 = 2 & J_1 = J_2 = 1 \\ a_j^* = 1000 & b_j^* = \frac{2a_j^*}{\pi} & c_j^* = 10 & \xi_i = 0.1 \qquad \text{with } j = 1 \ldots 4. \end{array}$$

The starting/initial position is $(q_1(0); \dot{q}_1(0); q_2(0); \dot{q}_2(0)) = (0; 0; 0; 0)$, the targeted one $(q_1(0); \dot{q}_1(0); q_2(0); \dot{q}_2(0)) = (0.8; 0; 0; 0)$. This means, the first segment of the arm is moving 0.8 rad counterclockwise, the second segment shall hold its position.

Simulation 1: The results of the first simulation are shown in Figs. 2 and 3 which present the system behavior. Here, we use the conventional PID-controller (3) with the parameters:

$k_{P1} = 80 \quad k_{D1} = 180 \quad k_{I1} = 70$
$k_{P1} = 500 \quad k_{D1} = 100 \quad k_{I1} = 300$

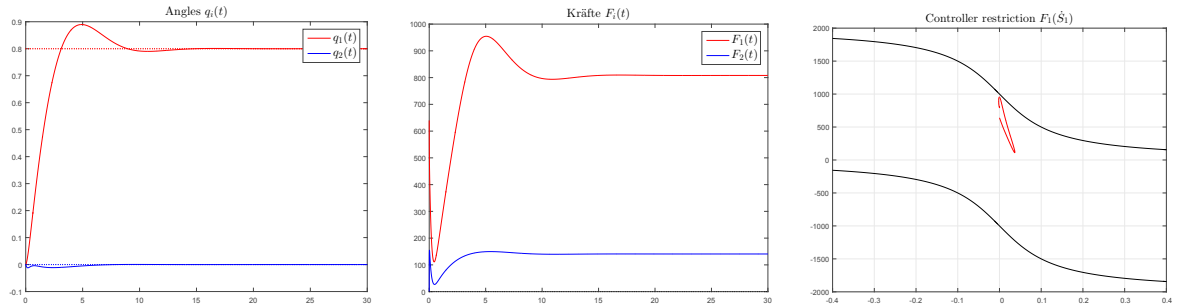

Figure 2. Simulation 1: joint angles (left), forces (middle), controller restriction of first joint (right).

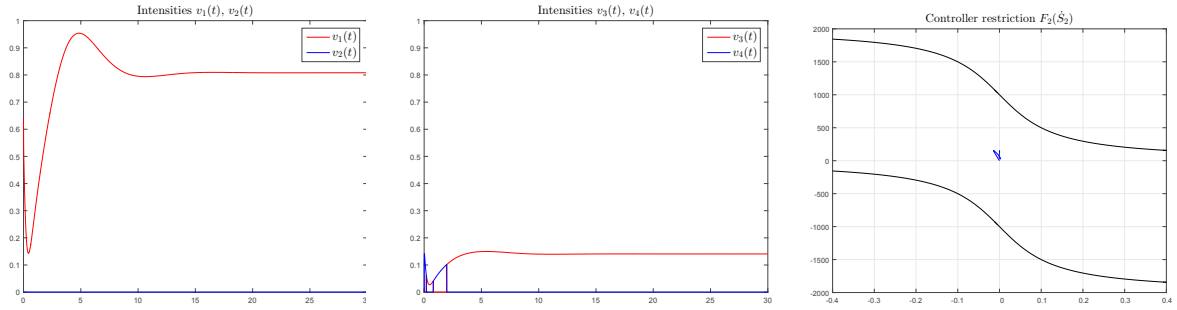

Figure 3. Simulation 1: intensities of muscles C_{C1}, C_{C2} (left), Intensities of muscles C_{C3}, C_{C4} (middle), controller restriction of second joint (right).

The control parameters of the first segment has to be chosen quite low, for not to leave the restriction area on their own. The ones for the second segment can be chosen high, because this one has only to stabilize itself. The chosen parameters for segment 1 are nearly on the limit to leave the controller restriction area.

Simulation 2: The result shown in Figs. 4 and 5 offer higher control parameters for segment 1 and show what happens when the saturation of the control variable appears. The chosen parameters are:

$k_{P1} = 200 \quad k_{D1} = 300 \quad k_{I1} = 200$
$k_{P1} = 500 \quad k_{D1} = 100 \quad k_{I1} = 300$

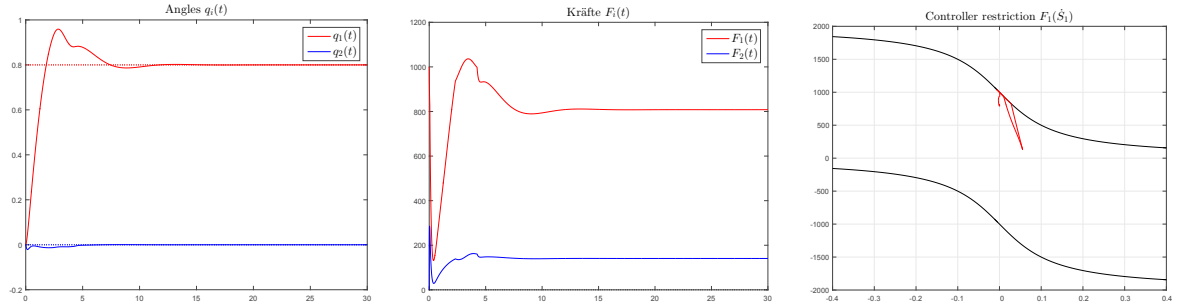

Figure 4. Simulation 2: joint angles (left), forces (middle), controller restriction of first joint (right).

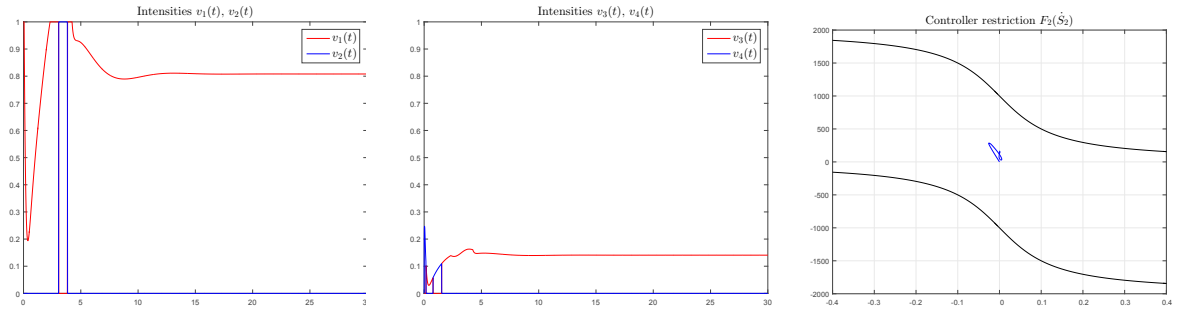

Figure 5. Simulation 2: intensities of muscles C_{C1}, C_{C2} (left), Intensities of muscles C_{C3}, C_{C4} (middle), controller restriction of second joint (right).

In the moment when the system requires more force to move the arm counterclockwise, the controller does not grant this. So, a higher overshoot with less control of the segment moving results. The conventional PID-controller (3) does not get on with its restriction.

Simulation 3: With the adaptive control strategies the restriction area can be exploit much better. In the following simulation presented in Figs. 6 and 7 the following control parameters are used for controller (4):

$\lambda_1 = 0.026 \quad \gamma_1 = 1200 \quad \kappa_1 = 0.5 \quad \eta_1 = 0.5$
$\lambda_2 = 0.026 \quad \gamma_2 = 600 \quad \kappa_2 = 0.5 \quad \eta_2 = 0.5$

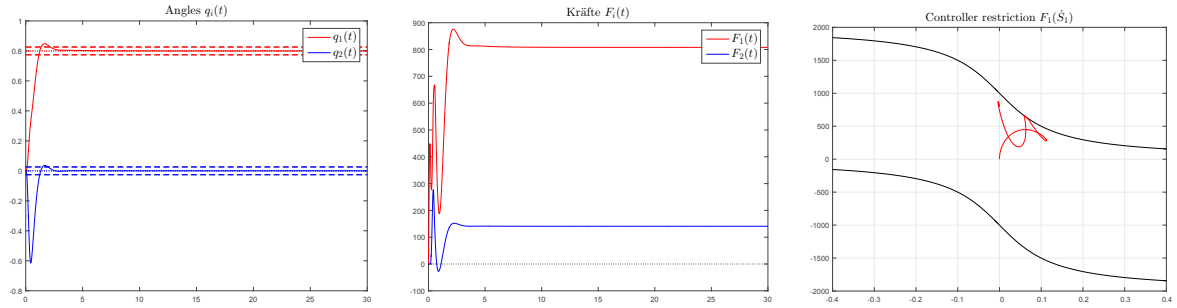

Figure 6. Simulation 3: joint angles (left), forces (middle), controller restriction of first joint (right).

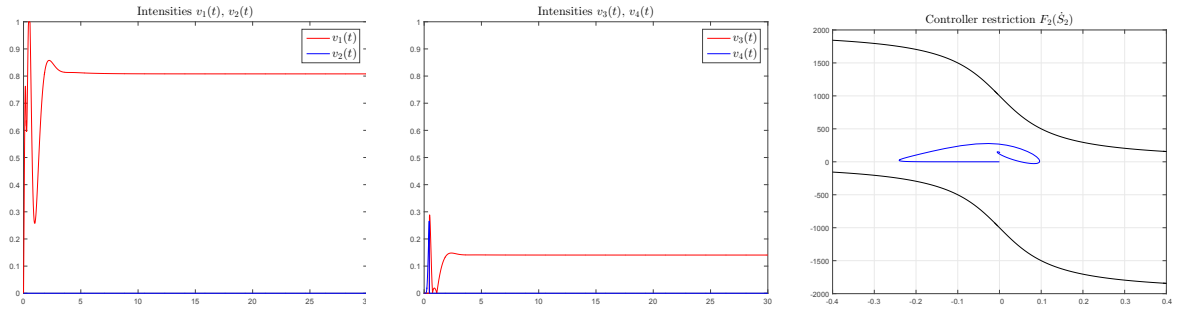

Figure 7. Simulation 3: intensities of muscles C_{C1}, C_{C2} (left), Intensities of muscles C_{C3}, C_{C4} (middle), controller restriction of second joint (right).

The results show from the beginning, that the intensity v_1 shoots up to its maximum and touches the controller restriction limit. Additionally, the targeted angles are reached much faster and more precisely than in Simulation 2. The controller determines the needed gain factors on its own, so it is not such stiff as the PID-Controller before.

Simulation 4: Still one big disadvantage is present: The gain factor cannot be reduced. After several arm movements the controller will still stay at very high gain factors, so that all movements will be done with "full" power. One solution is the advanced λ-stabilization (5). Its performance is shown in the simulation results of Figs. 8 and

9, using the following control variables:

$\lambda_1 = 0.026 \quad \varepsilon_1 = 0.7 \quad \gamma_1 = 640 \quad \kappa_1 = 0.5 \quad \eta_1 = 0.2 \quad \sigma_1 = 0.2 \quad t_{d1} = 2$

$\lambda_2 = 0.026 \quad \varepsilon_2 = 0.7 \quad \gamma_2 = 400 \quad \kappa_2 = 0.5 \quad \eta_2 = 0.2 \quad \sigma_2 = 0.2 \quad t_{d2} = 2$

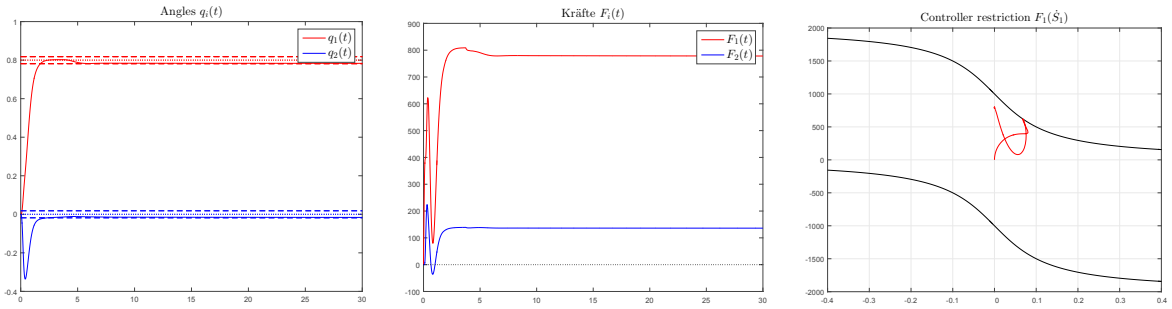

Figure 8. Simulation 4: joint angles (left), forces (middle), controller restriction of first joint (right).

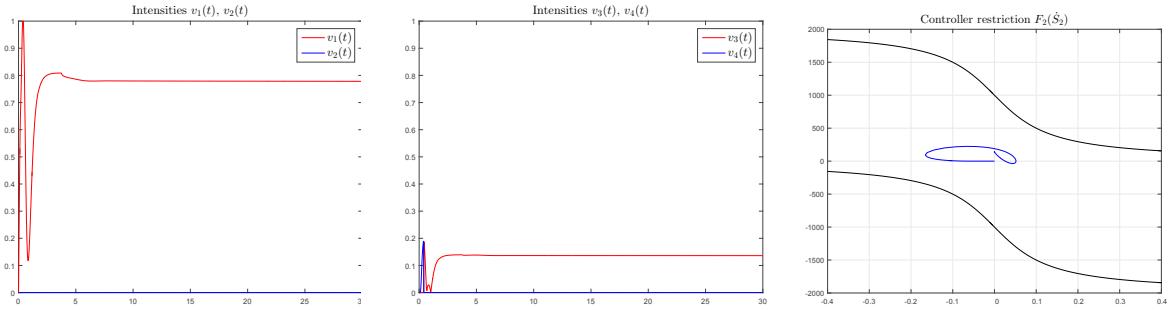

Figure 9. Simulation 4: intensities of muscles C_{C1}, C_{C2} (left), Intensities of muscles C_{C3}, C_{C4} (middle), controller restriction of second joint (right).

The simulation shows a very good stabilization of the targeted position. Because of the falling gain factor, the angle q_1 is positioned on the limit of the λ-tolerance area. After enough time the gain factor is reduced too much, so the angle leaves the tolerance area what the controller leads to rise up and start the process again.

Simulation 5: The last simulation shows the behavior of the saturated controller (6). The best results of this one were even found in [1], these simulation results – shown in Figs. 10 and 11 – are presented to compare them with the results above.

$k_{1\,1} = 0 \quad k_{2\,1} = 1$

$k_{1\,2} = 0 \quad k_{2\,2} = 1$

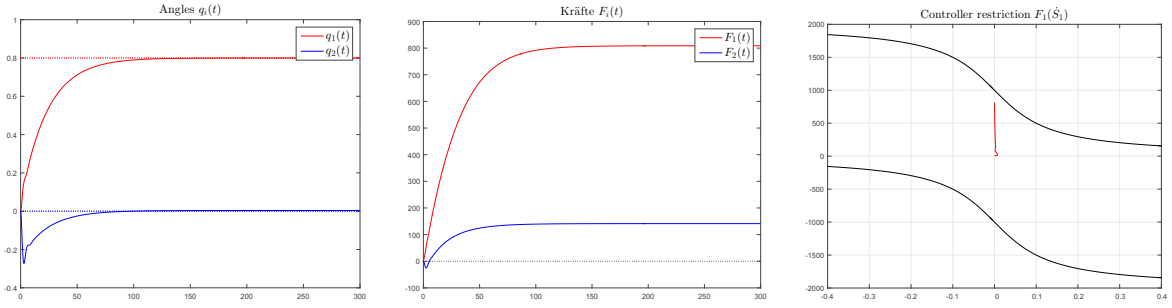

Figure 10. Simulation 5: joint angles (left), forces (middle), controller restriction of first joint (right).

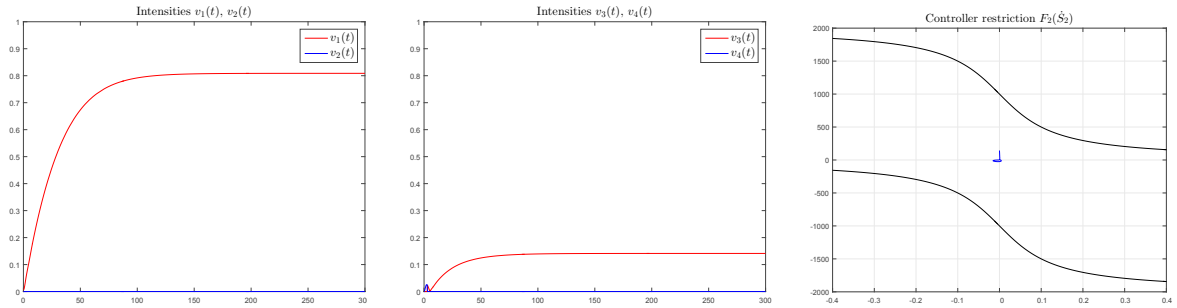

Figure 11. Simulation 5: intensities of muscles C_{C1}, C_{C2} (left), Intensities of muscles C_{C3}, C_{C4} (middle), controller restriction of second joint (right).

The simulation shows a precise stabilization of the targeted position, without inappreciable overshoots. The problem of this control strategy is its velocity: it is about ten times slower than on the shown control strategies above. This can be solved by a trial&error-method in adjusting the control parameters, which is unfavorable.

6. CONCLUSIONS

Starting with the introduction of the model and the derivation of the equations describing the dynamics, we presented several control strategies to be applied to the muscle-like compliant robotic system in order to stabilize a set point. Due to the lack of the precise knowledge of system parameters, the focus was on adaptive control schemes. Because of the natural behavior of the used muscle structures as unconventional control input variables (muscle force), we set up several problems and solve them: converting necessary control torques in muscle forces, using the angular velocities which had to be converted into contraction velocities of the muscles. The last problem was to guarantee a saturated control input the determine valid intensities for controlling the muscles.
The simulations carried out showed the effectiveness of the proposed advanced λ-tracking PID-controller, compared to the other control strategies. This controller fulfilled the stabilization process in a very short time with high precision. Because of its adaptive nature it is universal in combination with a hard saturation.

7. REFERENCES

[1] Abeßer H., Behn C., Steigenberger J., Zimmermann K. (2002): Steueraufgaben für Zweiarm-Roboter mit muskelähnlichen Antrieben; in *Proc. 47. International Scientific Colloquium*, Ilmenau.

[2] Awrejcewicz J., Reshmin S.A., Wasilewski G., Kudra G. (2008): Swing up a double pendulum by simple feedback control; in *Proceedings ENOC 2008*, St. Petersburg, Russia.

[3] Behn C. (2005): *Contributions to the adaptive control of bio-inspired systems*; Cuvillier, Göttingen.

[4] Behn C. (2013): Mathematical Modeling and Control of Biologically Inspired Uncertain Motion Systems with Adaptive Features; Habilitation thesis, Dept. of Mechanical Engineering, TU Ilmenau.

[5] Behn C., Loepelmann P., Steigenberger J. (2015): Analysis and simulation of adaptive control strategies for uncertain bio-inspired sensor systems: *Mathematics In Engineering, Science and Aerospace (MESA)* 6(3), pp. 567–588.

[6] Gluck T., Eder A., Kugi A. (2013): Swing-up control of a triple pendulum on a cart with experimental validation; *Automatica* 49(3), pp. 801-–808.

[7] Ortega R., Loría A., Nicklasson P.J., Sira-Ramírez H. (1998): *Passivity-based Control of Euler-Lagrange Systems*; Springer, London.

[8] Schmalz T. (1993): *Biomechanical Modeling of Human Motion*; Hofmann-Verlag, Schorndorf.

[9] Siedler K. (2017): Numerische und experimentelle Verifikation von adaptiven Regelungsstrukturen an einem mechatronischen, nachgiebigen System; Master thesis, TU Ilmenau, Ilmenau.

[10] Siedler K., Behn C. (2017): Adaptively Controlled Dynamical Behavior of Sensory Systems based on Mechanoreceptors; *International Journal of Structural Stability and Dynamics*, in press, DOI: http://dx.doi.org/10.1142/S0219455417400028

[11] Wagner H., Blickhan R. (1999): Stabilizing Function of Skeletal Muscles: an Analytical Investigation, *J. theor. Biol.*, pp. 163–179.